Multimaterial 3D printing of biocomposite materials

Kayah St. Germain, Hani E. Naguib, Damien Marchand, Médéric Morisset, Laurence Chocinski-Arnault, Fabienne Touchard

MULTIMATERIAL 3D PRINTING OF BIOCOMPOSITE MATERIALS

Kayah St. Germain[1,2], Hani E. Naguib[1], Damien Marchand[2], Mederic Morisset[2], Laurence Chocinski-Arnault[2] and Fabienne Touchard[2]

[1]University of Toronto, Mechanical and Industrial Engineering, 27 King's College Cir, M5S 1A1 Toronto, ON, Canada
Email: kayah.stgermain@mail.utoronto.ca, hani.naguib@mail.utoronto.ca, Web Page: https://tsmart.mie.utoronto.ca/
[2]Institut Pprime, Dpt Physique et Mécanique des Matériaux, CNRS-ENSMA-Université de Poitiers, 1 av. C. Ader, B.P. 40109, 86961 Futuroscope Chasseneuil, France
Email: damien.marchand@ensma.fr, mederic.morisset@ensma.fr, laurence.chocinski@ensma.fr, fabienne.touchard@ensma.fr, Web Page: https://pprime.fr/en/home-pprime/

Keywords: Biocomposite, 3D-Printing, Multimaterial Printing, Wettability, Compression

Abstract

Additive manufacturing is a promising and disruptive technology that is being applied in many industrial sectors, such as aeronautics, robotics, and bioengineering, because of the ease of use and high level of customizability that it offers. Additionally, biocomposite materials are being seen incorporated more frequently in industry because of favourable properties such as being recyclable, biocompatible, biodegradable, having low environmental impact, and comprising of naturally abundant materials. In this study, multimaterial 3D printing involving a PLA/hemp biocomposite and pure PLA was done, with the focus being on keeping the bulk of the part as the biocomposite material and adding a PLA covering to the outer surface to explore the compatibility of the two materials being printed together and the effect on the mechanical properties. Contact angle measurements and immersion testing were done to see the effect of the hemp biofiller on the way the PLA interacts with moisture and compression testing was done to compare the performance of the samples in a dry and wet state. Optical and x-ray imaging techniques were used to closely examine the final printed specimens and give insight to the results of the testing.

1. Introduction

As wider industry aims to become more sustainable to reduce environmental impact and lasting damage, biocomposites are being looked to more and more as an alternative to traditional manufacturing materials. Natural fibers, such as the hemp fibers being studied here, are of increasing interest for being naturally abundant, a renewable resource, requiring little energy to produce, their potential to replace synthetic fibers in the fabrication of composite materials, and favourable properties such as durability and flexibility [1, 2]. When paired with a biodegradable polymeric matrix, they also make fabricated parts easier to recycle and more environmentally friendly to produce and dispose of [3].

Alongside this industrial push for more sustainable materials, there has also been increased interest in 3D printing and its potential use in industry due to advantages over traditional manufacturing techniques such as increased design flexibility, the ability to accommodate complex geometries more easily, and the decreased amount of waste material produced, especially when compared to subtractive manufacturing techniques [4]. To continue to reduce the environmental footprint of 3D printing technologies, there has been the development of biocomposite 3D printing filament.

In this study, a commercially available hemp/polylactic acid (hPLA) biocomposite filament and a pure polylactic acid (PLA) filament will be characterized then samples of the two together will be fabricated using multimaterial 3D printing to examine their compatibility and resulting physical properties. Comparing the PLA and hPLA directly allows us to easily identify the effect of the hemp on the material properties and, further, the possibilities for combining the two materials together. Because the preference is for the bulk material to remain the biocomposite, the PLA was added to an hPLA cube in only a thin layer covering the outside so that the entirety of the hPLA was encapsulated but still using the minimum amount of PLA possible.

2. Materials and Methods

2.1. Sample Materials

The samples were fabricated using an Ultimaker S5 fused deposition modeling (FDM) multimaterial 3D printer and used as printed without any additional post processing or modifications. The specifications for the two filaments used can be found in Table 1.

Table 1. Properties of 3D printer filaments

Material	Filament Diameter	Tensile Stress at Yield	Print Temperature	Build Plate Temperature	Hemp weight %	Supplier
hPLA	2.85mm	16MPa	210°C	60°C	≤10	3D-Fuel
Tough PLA	2.85mm	37MPa	225°C	60°C	0	Ultimaker

2.2. Sample Analysis

Two types of imaging were used on the samples for different purposes. To examine the surface topography created through the 3D printing process on the different faces of the single material samples, an Alicona Infinite Focus optical 3D measuring tool was used. These images were correlated to the wetting behaviour of the surfaces through comparison with the measured contact angles. Tomography X-ray imaging for the multimaterial samples was done using an UltraTom CT scanner from RX Solution. Getting images throughout the entire thickness of the sample revealed the interface regions between the two materials, the effectiveness of the adhesion between layers, the printing quality, and any defects present as a result of the fabrication process.

2.3. Contact Angle Measurements

Contact angle measurements were taken using an Ossila Contact Angle Goniometer at approximately 20°C and 40% humidity room conditions. The surface of the sample was cleaned with ethanol to remove any contaminants or dust then left untouched for an adequate amount of time to ensure any leftover ethanol had evaporated from the surface and would not influence the measurement. A droplet of distilled water was placed on the surface and allowed to settle with the measurement taken within 15 seconds of the droplet being placed to mitigate the possible effect of external factors that could unintentionally influence the measurement with time (ex. vibration or evaporation).

2.4. Immersion Experiment Set-Up

Moisture absorption analysis was conducted on the 3D printed samples for each of the materials. The printed samples were dehydrated in a 60°C oven for 24 hours and their initial masses were recorded. They were then fully immersed in deionized water and removed periodically over the span of the experiment to have their new mass recorded. Measurements were taken using an electronic scale with excess water being removed from the outside of the sample with a paper towel and compressed air as needed before having the measurement taken and being returned to the water. Equation (1) was used to calculate the percent change in mass and these values were graphed to monitor the trend in absorption over time.

$$M(\%) = \frac{M_s - M_i}{M_i} \times 100 \quad (1)$$

where M is the percent change in mass from moisture absorbed, M_s is the mass of the sample at the point in time that it is removed from the water in grams, and M_i is the initial mass of the sample in grams.

2.5. Compression Testing

Compression testing was performed on the samples to test their mechanical performance. The compression testing was performed using an Instron 5982 machine at a rate of 1mm/min. The testing was conducted on all the samples in both a dry and wet (after being immersed in water) state with the wet measurements being done immediately after the samples were removed from the water they were immersed in.

3. Results

3.1 Sample Preparation

Two different types of samples were analyzed, the first being single material samples and the second being multimaterial samples. The initial comparison and characterization of the hPLA and PLA base materials was done using 10mmx10mmx10mm 3D printed cubes fabricated using the printer settings found in Table 2 and can be seen in Figure 1a).

Table 2. Printer specifications for single material cube samples

Specification	Value
Z resolution (layer thickness)	0.2mm
XY resolution (nozzle diameter)	0.8mm
Infill Pattern	Lines
Infill Orientation	90 degrees
Infill Density	100%
Slicer Software	Cura

For the multimaterial samples, the 10mmx10mmx10mm hPLA cubes were printed with a 0.4mm thick pure PLA outer layer using the printer settings found in Table 3. Figure 1b) shows a cross section of one of the samples where the inner hPLA cube and outer PLA coating can be seen.

Table 3. Printer specifications for multimaterial cube samples

Specification	hPLA	PLA
Z resolution (layer thickness)	0.2mm	0.2mm
XY resolution (nozzle diameter)	0.8mm	0.4mm
Top/Bottom Thickness	n/a	0.4mm
Wall Thickness	n/a	0.4mm
Infill Pattern	Lines	n/a
Infill Orientation	90 degrees	n/a
Infill Density	100%	n/a
Slicer Software	Cura	Cura

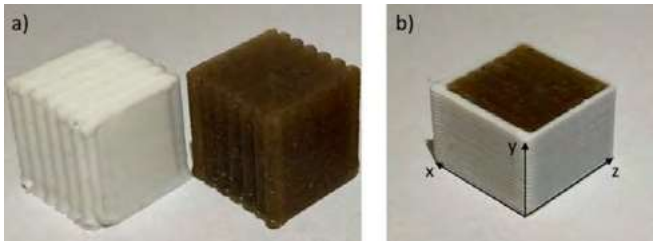

Figure 1 a) PLA (white) and hPLA (brown) single material cube samples b) Cross section of PLA covered hPLA cube fabricated using multimaterial 3D printing

3.2. Surface Morphology

Because of the layer-by-layer filament deposition technique that is used in FDM 3D printing, the fabrication process results in a number of different macroscopic microscale surface patterns. Optical images were taken of three different hPLA cube faces. The top surface (Figure 2a)) contains wide valleys divided by sharp peaks that were caused by the extrusion nozzle dragging across the surface when depositing the topmost layer of the part. The side face (Figure 2b)) contains the most regular structuring, with 0.2mm wide rounded peaks divided by sharp valleys created by the layers of the filament building up the part. The bottom face (Figure 2c)), having been in contact with the glass of the printer bed, was left with the smoothest finish, but thin line indents formed by the winding of the filament deposition were still visible. In all three cases, the pattern is not completely symmetrical and there is a clear directionality caused by the filament deposition. The variations in the surface patterning exhibited by each face influences the wettability which will be seen in the following section through the contact angles.

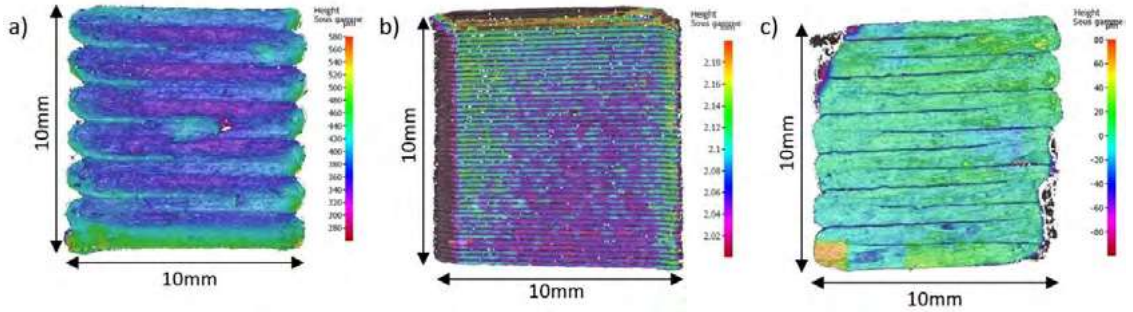

Figure 2. Alicona optical microscope topography images of the a) top face of the hPLA cube b) side face of the hPLA cube c) bottom face of the hPLA cube

3.3. Contact Angles

To compare the surface wettability of the two materials, the static water contact angle was measured on the three different faces of the cube samples. The measurements for the droplet on the surface were taken from two different perspectives, as shown in Figure 3, to get a view of the anisotropy caused by the directionality of the lined surface texture with results graphed in Figure 4. Broadly comparing the performance of the two materials, the same trend can be found regarding the contact angles for all sides in all directions, that being that the hPLA exhibited a notably lower contact angle than the PLA. This is in agreement with what is to be expected given that the addition of hydrophilic hemp fibers [5] to the PLA should result in a more hydrophilic surface and decrease in contact angle. With the biocomposite filament used in this study having a max filler weight percentage of only 10% and the contact angle already being lowered by approximately 10 degrees when compared to pure PLA, it suggests that as the weight percentage of the biofiller continues to be increased, it will largely increase the wettability of the surface.

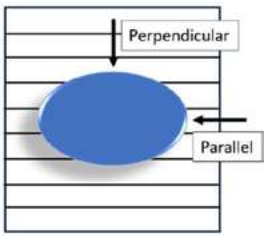

Figure 3: Top view of anisotropic water droplet

The effect of the line pattern on the contact angle can also be seen on all faces, with the difference for each face in the parallel and perpendicular direction being close to or more than 10 degrees, classifying the surface behaviour as anisotropic [6]. This is because the water droplet prefers to spread in the direction of the continuous lines, which offer little to no resistance to motion, causing wider spreading and a lower contact angle in the direction of the filament [7, 8]. Figure 4b) shows that the side face of the cube, which is the most heavily textured, achieves the most extreme contact angles and displays the most anisotropy. The other two faces, with their similar, less defined surface patterns, have lower and more comparable angles in the two directions. Comparing the three sides clearly shows the way that different patterning influences the way water interacts with a surface.

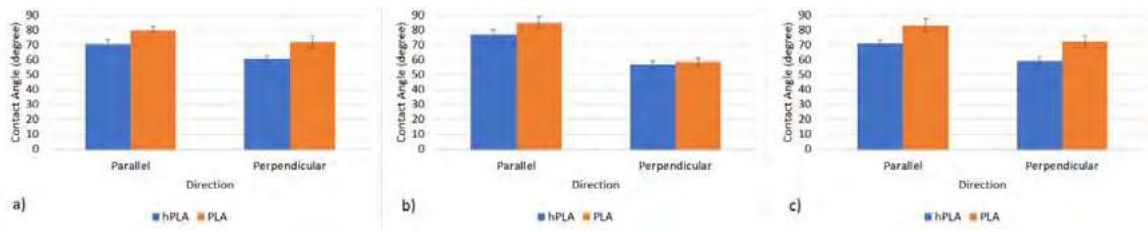

Figure 4. Water contact angles of the a) top face with nozzle pattern b) side face with layer pattern c) bottom face in contact with build plate

3.4. Cube Immersion

Looking past the surface of the material, the bulk material was also studied through fully immersing the single material cube samples in water to monitor their absorption behaviour. Two samples of each material were included in the experiment to see the repeatability and consistency of the results. The majority of the water absorption done by the PLA cube took place within the first 24 hours of the experiment before slowing down and plateauing at 1.147 ± 0.058 weight percent after 14 days. The absorption behaviour of the hPLA was different from that of the PLA, with the water absorption happening more gradually over a more extended period of time and eventually resulting in a higher percent change in mass at 1.99% ± 0.27 after 34 days.

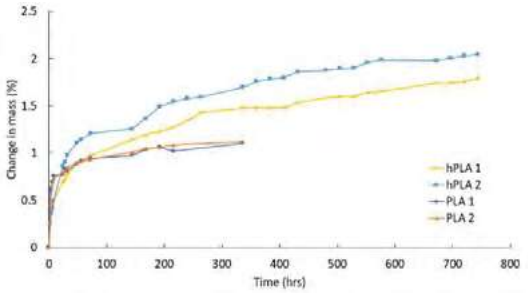

Figure 5. Water absorption over time for two hPLA samples and two PLA samples

Comparing the immersion results from the two materials, the hPLA is found to be more hygroscopic than the PLA, again, due to the addition of the hemp fibers. Hydrophilic natural fibers are inherently prone to moisture absorption [9], with their influence clearly seen when comparing the results of the hPLA to the pure PLA. The inclusion of a filler in the polymer matrix means that instead of water only diffusing through the microgaps in the polymer chains, it can also now penetrate through capillary transport at flaws in the fiber-matrix interfaces, and through microcracks in the matrix caused by the swelling of the fibers, a large problem with biofillers specifically when compared to synthetic fillers [10, 11]. Moisture absorption triggered by the addition of natural fibers will only continue to increase as the weight percentage of the filler in the composite is further increased [12, 13], leading to a faster degradation of the mechanical properties and the fibers themselves. Additionally, it was observed that the absorption exhibited by the two PLA samples was almost identical whereas there was a larger difference in the amount of the absorption that took place between the two hPLA samples, with one at 1.79wt% and the other at 2.1wt%. A possible explanation for this is that natural fibers tend to have different lengths and widths [14] or could possibly not be uniformly distributed throughout the composite, making its behavior more varied and unpredictable.

3.5. Compression Testing

Compression testing was conducted on the single material hPLA and PLA cubes as well as on the hPLA cube with the PLA outer layer in both a dry state and after having been immersed in water. A number of observations can be made from the generated stress-strain curves in comparing the materials to each other and comparing their dry and wet counterparts. Figure 6 compares the compression results for the three different cube samples in the dry state. The hPLA was able to withstand larger compressive loads than the PLA and exhibited a larger compressive modulus. This indicated that the addition of hemp fibers had a positive effect on improving the mechanical performance of the PLA. The multimaterial cube did not perform as well as the hPLA cube but did perform significantly better than the PLA cube in resisting compressive loading.

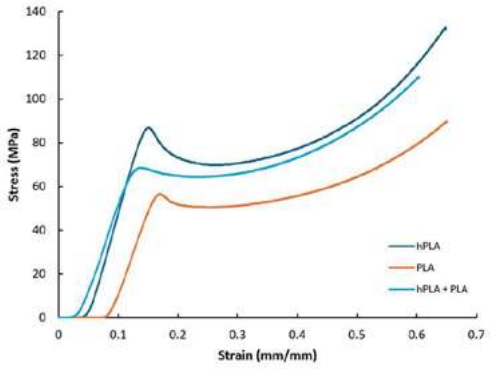

Figure 6. Stress-strain curves generated from compression testing for the single and multimaterial samples in a dry state

Comparing the performance of the three different samples in compression before and after being immersed in water showed some interesting trends with which samples were affected by hydroplasticization and how. After being immersed in water, there was no sign of hydroplasticization and little change in the mechanical performance of the PLA, with both curves in Figure 7a) being almost identical. A similar observation was made by Banjo et al. who performed flexural testing on 3D printed PLA samples and found little change between samples that were dry and those that had been immersed in water [15]. After the hPLA was immersed, the compressive strength of the sample decreased due to the hydroplasticization of the material induced by the increased moisture absorption from the presence of the hemp fibers. It is also likely that the moisture absorption weakened the interfaces between the polymer matrix and the hemp fibers, reducing their ability to reinforce the composite [16]. The hydroplasticization is indicated by the difference in shape between the dry and wet curve seen in Figure 7b), with the stress softening phase being completely eliminated and the sharp peak of the yield strength lessening. Hydroplasticization most effects polar materials and natural fibers are largely polar meaning their addition to PLA promotes the effect, causing the different reactions of PLA and hPLA to the long-term immersion [17]. Hydroplasticization leading to a reduction in hardness and increase in ductility in biocomposite materials is a phenomenon that has been widely reported in literature in the past [18, 19, 20, 21]. The multimaterial PLA covered hPLA cube showed signs of plasticization, consistent with the hPLA sample, but not a decrease in mechanical performance, consistent with the PLA sample. Because the outside PLA covering was not completely watertight, it is likely that water penetrated through to and was absorbed by the hPLA, causing plasticization of the inner hPLA portion. Contrarily, the unaffected PLA could have counteracted the loss in compressive strength caused by the plasticization of the hPLA, resulting in no change in the yield strength or modulus after immersion.

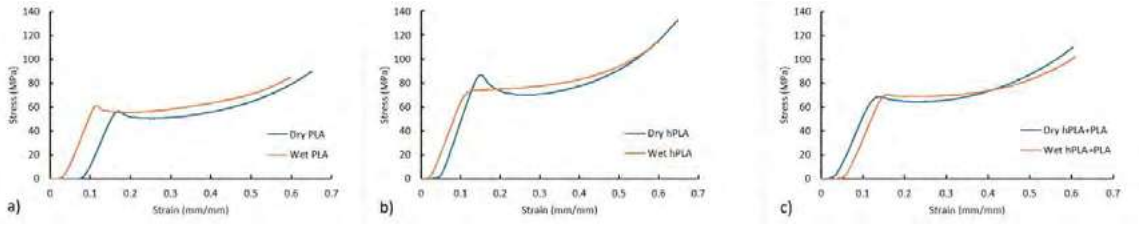

Figure 7. Stress-strain curves comparing the performance of the dry and wet samples for a) PLA b) hPLA and c) hPLA with PLA on the outside

3.6. Tomography Images

Tomography imaging revealed that throughout the multimaterial cube sample the printing quality could vary, with some influencing factors being the compatibility between the two materials, the alignment of the printer, and the deposition process itself. The images showed that defects can occur not only at the interfaces between two different materials but also within the layers of a single material based on the deposition of the filaments and the adhesion between layers. The quality of the adhesion at the interface between the two materials also varies based on which side of the cube sample you are considering. Figure 8a) and b) show highly visible gaping that exists between two different material layers along the entire length of one side. In the case of Figure 8a), on the lefthand side of the image, the cross section of the deposited filaments can be seen and there exists a clear gap between the outermost layer and the following layer. Comparing the image to the CAD model, Cura model, and actual sample showed that this space was likely created because of the deposition path chosen by the slicing software which was different than that taken for all the other sides. Figure 8b) shows the same gap but from the top view in the layer direction. In Figure 8c), thin slits formed between the layers of the hPLA in the centre cube structure can be seen. These types of porosities are typical in 3D printed parts and represent slights areas where two layers did not completely and uniformly fuse together.

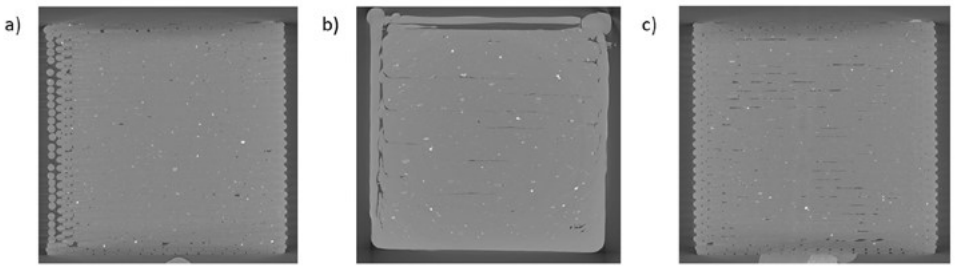

Figure 8: Tomography images of PLA covered hPLA cube taken from the a) x-direction b) y-direction c) z-direction

4. Conclusions

In this study, hemp/PLA biocomposite filament was studied to see the effect of the hemp fiber biofiller on the material properties along with the possibility of using multimaterial 3D printing to reinforce the biocomposite with an outside layer of pure PLA. The addition of the hemp to the PLA matrix made the material both more hydrophilic and hygroscopic, making water more likely to adsorb to the surface as well as absorb into the bulk. The hemp fibers were also seen to enhance the compressive strength of the PLA when dry, but the increased moisture absorption caused more significant plasticization of the material and a decrease in compressive strength after being immersed in water. With the use of multimaterial 3D printing, a shell of PLA was able to be added to completely encapsulate the biocomposite. It was found that these materials were largely compatible to be printed alongside one another with the multimaterial part, in most cases, showing good adhesion at the interfaces between the two. The multimaterial sample also showed that after being immersed in water, there was evidence of plasticization having occurred in the hPLA but there was not any observed decrease in the compressive strength, likely due to the continued integrity of the outer PLA. These results are promising for the future use of biocomposites in humid or moist environments and the possibility of using slight amounts of PLA as a reinforcing material to overcome some of the pitfalls of biofiller incorporation while preserving the integrity of the biodegradability and biocompatibility.

Acknowledgements

The authors would like to thank Institut Pprime and CNRS-ENSMA-Université de Poitiers for the use of their research facilities and support from their personnel, specifically David Mellier and Amelie Caradec, in conducting this research. The authors would also like to acknowledge the financial support provided by Mitacs and the University of Toronto for this research.

References

[1] M. J. John and S. Thomas, "Biofibres and biocomposites," *Carbohydrate Polymers*, vol. 71, no. 3. pp. 343–364, Feb. 08, 2008. doi: 10.1016/j.carbpol.2007.05.040.

[2] G. W. Beckermann and K. L. Pickering, "Engineering and evaluation of hemp fibre reinforced polypropylene composites: Fibre treatment and matrix modification," *Compos Part A Appl Sci Manuf*, vol. 39, no. 6, pp. 979–988, Jun. 2008, doi: 10.1016/j.compositesa.2008.03.010.

[3] A. Mtibe, M. P. Motloung, J. Bandyopadhyay, and S. S. Ray, "Synthetic Biopolymers and Their Composites: Advantages and Limitations—An Overview," *Macromolecular Rapid Communications*, vol. 42, no. 15. John Wiley and Sons Inc, Aug. 01, 2021. doi: 10.1002/marc.202100130.

[4] W. Gao *et al.*, "The status, challenges, and future of additive manufacturing in engineering," *CAD Computer Aided Design*, vol. 69, pp. 65–89, Dec. 2015, doi: 10.1016/j.cad.2015.04.001.

[5] S. L. Schellbach, S. N. Monteiro, and J. W. Drelich, "A novel method for contact angle measurements on natural fibers," *Mater Lett*, vol. 164, pp. 599–604, Feb. 2016, doi: 10.1016/j.matlet.2015.11.039.

[6] K. M. Lee, H. Park, J. Kim, and D. M. Chun, "Fabrication of a superhydrophobic surface using a fused deposition modeling (FDM) 3D printer with poly lactic acid (PLA) filament and dip coating with silica nanoparticles," *Appl Surf Sci*, vol. 467–468, pp. 979–991, Feb. 2019, doi: 10.1016/j.apsusc.2018.10.205.

[7] C. J. Long, J. F. Schumacher, and A. B. Brennan, "Potential for tunable static and dynamic contact angle anisotropy on gradient microscale patterned topographies," *Langmuir*, vol. 25, no. 22, pp. 12982–12989, Nov. 2009, doi: 10.1021/la901836w.

[8] D. Xia and S. R. J. Brueck, "Strongly anisotropic wetting on one-dimensional nanopatterned surfaces," *Nano Lett*, vol. 8, no. 9, pp. 2819–2824, Sep. 2008, doi: 10.1021/nl801394w.

[9] A. Shahzad, "Hemp fiber and its composites - A review," *J Compos Mater*, vol. 46, no. 8, pp. 973–986, Apr. 2012, doi: 10.1177/0021998311413623.

[10] H. N. Dhakal, Z. Y. Zhang, and M. O. W. Richardson, "Effect of water absorption on the mechanical properties of hemp fibre reinforced unsaturated polyester composites," *Compos Sci Technol*, vol. 67, no. 7–8, pp. 1674–1683, Jun. 2007, doi: 10.1016/j.compscitech.2006.06.019.

[11] Z. N. Azwa, B. F. Yousif, A. C. Manalo, and W. Karunasena, "A review on the degradability of polymeric composites based on natural fibres," *Materials and Design*, vol. 47. Elsevier Ltd, pp. 424–442, 2013. doi: 10.1016/j.matdes.2012.11.025.

[12] A. Espert, F. Vilaplana, and S. Karlsson, "Comparison of water absorption in natural cellulosic fibres from wood and one-year crops in polypropylene composites and its influence on their

mechanical properties," *Compos Part A Appl Sci Manuf*, vol. 35, no. 11, pp. 1267–1276, Nov. 2004, doi: 10.1016/j.compositesa.2004.04.004.

[13] N. H. I. Kamaludin, H. Ismail, A. Rusli, and S. S. Ting, "Thermal behavior and water absorption kinetics of polylactic acid/chitosan biocomposites," *Iranian Polymer Journal (English Edition)*, vol. 30, no. 2, pp. 135–147, Feb. 2021, doi: 10.1007/s13726-020-00879-5.

[14] P. Sahu and M. K. Gupta, "A review on the properties of natural fibres and its bio-composites: Effect of alkali treatment," *Proceedings of the Institution of Mechanical Engineers, Part L: Journal of Materials: Design and Applications*, vol. 234, no. 1. SAGE Publications Ltd, pp. 198–217, Jan. 01, 2020. doi: 10.1177/1464420719875163.

[15] A. D. Banjo, V. Agrawal, M. L. Auad, and A. D. N. Celestine, "Moisture-induced changes in the mechanical behavior of 3D printed polymers," *Composites Part C: Open Access*, vol. 7, Mar. 2022, doi: 10.1016/j.jcomc.2022.100243.

[16] H. N. Dhakal, Z. Y. Zhang, N. Bennett, A. Lopez-Arraiza, and F. J. Vallejo, "Effects of water immersion ageing on the mechanical properties of flax and jute fibre biocomposites evaluated by nanoindentation and flexural testing," *J Compos Mater*, vol. 48, no. 11, pp. 1399–1406, 2014, doi: 10.1177/0021998313487238.

[17] J. G. Tsavalas and D. C. Sundberg, "Hydroplasticization of polymers: Model predictions and application to emulsion polymers," *Langmuir*, vol. 26, no. 10, pp. 6960–6966, May 2010, doi: 10.1021/la904211e.

[18] H. N. Dhakal, Z. Y. Zhang, N. Bennett, A. Lopez-Arraiza, and F. J. Vallejo, "Effects of water immersion ageing on the mechanical properties of flax and jute fibre biocomposites evaluated by nanoindentation and flexural testing," *J Compos Mater*, vol. 48, no. 11, pp. 1399–1406, 2014, doi: 10.1177/0021998313487238.

[19] C. P. L. Chow, X. S. Xing, and R. K. Y. Li, "Moisture absorption studies of sisal fibre reinforced polypropylene composites," *Compos Sci Technol*, vol. 67, no. 2, pp. 306–313, Feb. 2007, doi: 10.1016/j.compscitech.2006.08.005.

[20] A. Le Duigou, A. Bourmaud, P. Davies, and C. Baley, "Long term immersion in natural seawater of Flax/PLA biocomposite," *Ocean Engineering*, vol. 90, pp. 140–148, Nov. 2014, doi: 10.1016/j.oceaneng.2014.07.021.

[21] M. S. Islam, K. L. Pickering, and N. J. Foreman, "Influence of accelerated ageing on the physico-mechanical properties of alkali-treated industrial hemp fibre reinforced poly(lactic acid) (PLA) composites," *Polym Degrad Stab*, vol. 95, no. 1, pp. 59–65, Jan. 2010, doi: 10.1016/j.polymdegradstab.2009.10.010.